Kinematics of pulsating flow in the entry region of the channel with discrete roughness elements

Kinematics of pulsating flow in the entry region of the channel with discrete roughness elements

N S Dushin[1], N I Mikheev[1,2], A A Paereliy[1], I M Gazizov[2], R R Shakirov[2]

[1]Kazan Scientific Center of RAS
Russia, 420111 Kazan, Lobachevskogo str., 2/31
[2]Kazan National Research Technical University named after A N Tupolev - KAI
Russia, 420111 Kazan, K Marx str., 10

Abstract. One of the efficient ways to disrupt and redevelop the boundary layer for the purpose of heat transfer enhancement is application of discrete roughness elements in the form of spanwise ribs. To further improve the efficiency of this method, the flow can be exposed to some additional forcing. Forced pulsations of flow are considered to be a promising technique. The paper studies the combined effect of discrete roughness elements and forced pulsations of flow on heat transfer. Turbulent pulsating flow in the entrance region of the channel with discrete roughness elements has been considered. The Reynolds number based on the channel hydraulic diameter was Re_D = 18200, relative rib height e/h = 0.117, rib pitch p/e = 10. Strouhal number, Sr, and relative amplitude of forced velocity pulsations, β, varied in the following ranges: Sr = 0.04 … 0.6; β = 0.15 … 0.8. The Strouhal number was based on the bulk velocity and the rib height. Smoke visualization of flow downstream of the third rib in the channel has revealed the effects introduced by forced periodic pulsations to mass transfer behavior. The obtained flow behavior allowed qualitative and quantitative classification of the flow pattern.

1. Introduction

Modern approaches to heat transfer enhancement are based on turbulence promotion in the thin near-wall layer accompanied by moderate increase in the flow resistance. One of the efficient ways to arrange such flows is installation of discrete ribs in the channels. Optimal rib pitch in the steady regime in the Reynolds number range from 10^4 to 4×10^5 provides the enhancement of thermohydraulic performance by 26% [1]. Further augmentation of the heat transfer coefficient in rib-roughened channels can be attained by variation of the shape and position of ribs and by additional forcing of flow (flow rate pulsations, acoustic disturbance) [2 – 5]. External forcing of flow both enhances the heat transfer coefficient and moves its peak value closer to the ribs due to recirculation region reduction. Such regimes were observed in [4 – 9]. In particular, authors [6 – 9] note that the recirculation region reduced by an average of 30% compared to the steady flow case.

The review of papers dealing with separated pulsating flows showed that the majority of results have been obtained from DNS of fully developed flow, while the experimental papers are scarce and mainly consider the case of a single roughness element under certain combination of parameters of flow unsteadiness. This results from the complexity of measurements and more complex flow pattern in ribbed channels [5]. For example, authors [10] showed that disturbances generated by the rib persist far downstream of the latter and considerably affect the flow field around the next rib.

The measurements in unsteady flows are complex since time-resolved 2D or 3D techniques should be used. Such instruments have been developed recently (Time-resolved PIV [11], SIV [12, 13]). And until then, the measurements were performed using either single-point instruments (hot-wire anemometer, LDV), or 2D techniques (PIV, PTV) with averaging over the period of pulsation or snapping to the pulsation phase. Thus, the information required for advanced cooling system design could be obtained but it did not provide the detailed insight into the physics of flow.

The present paper elaborates on kinematic structure of turbulent flow unsteady with time in the entrance region of rib-roughened channel. Flow rate unsteadiness was generated by a rotating flap periodically blocking the test section outlet. High-speed video recording of smoke visualization was mainly used to analyze the flow. Quantitative characteristics of flow were estimated from SIV measurements.

The flow pattern between the third and fourth ribs was experimentally studied at the following parameters: the Reynolds number based on the channel hydraulic diameter, D_h, was Re_{Dh} = 18200; relative rib height e/h = 0.117, rib pitch p/e = 10. The dimensionless numbers were varied in the following ranges: Strouhal number Sr = 0.04 … 0.6; relative amplitude of forced velocity pulsations $\beta = u'/\overline{u}$ = 0.15 … 0.8. The Strouhal number was based on the bulk velocity and the rib height.

2. Experimental setup

Schematic of the experimental setup is shown in Figure 1. Its main components are the following: smoke preparation chamber *1*, measurement section *5*, pulsator *8*, receiver *9*, and suction fan *12*. The measurement section was a rectangular channel with the length of L=1.2 m and a cross section of 150×115 mm^2 made of transparent polycarbonate. Square aluminum ribs with the cross section of 13.5×13.5 mm^2 were mounted on the bottom wall of the measurement section. A two-dimensional smooth inlet *2* was located between the measurement section inlet and the smoke preparation chamber. The smooth inlet was shaped according to the Bernoulli lemniscates curve and had a contraction ratio of 5.5:1. To turbulize the flow and fix the point of laminar-turbulent transition, a turbulence generating grid *3* (made of wire with the diameter of 1.4 mm and spacing of 6 mm) was mounted at the measurement section inlet and a P24 abrasive *4* was glued to the channel perimeter. The pulsator *8* was installed between the measurement section outlet and the receiver [14]. Inside the pulsator there were two pass-through ducts with adjustable cross section. One of these ducts was equipped with a contoured rotating flap driven by an electric motor with frequency converter. Thus, flow pulsations with adjustable frequency and amplitude could be generated in the test section. The flow rate variation was close to harmonic law.

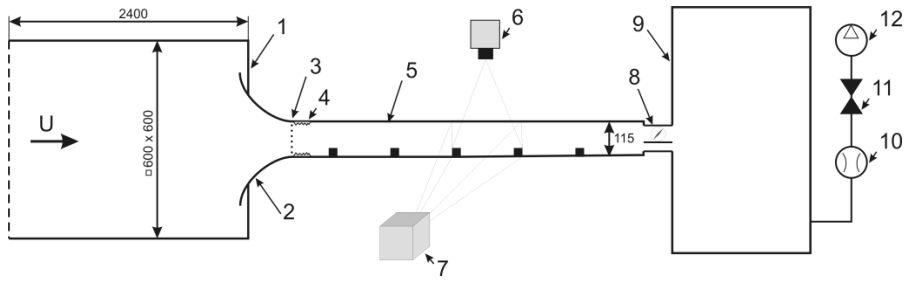

Figure 1. Schematic of experimental setup. *1* – smoke preparation chamber; *2* – smooth inlet; *3* – turbulence generating grid; *4* – abrasive; *5* – measurement section; *6* – DPSS laser; *7* – high-sped camera; *8* – pulsator; *9* – receiver; *10* – flow meter; *11* – ball valve; *12* – suction fan

Stability of the air flow rate through the measurement section was provided by the valves, receiver and suction fan characteristics. The volume flow rate was measured by an ultrasonic flow meter IRVIS-RS4-Ultra with the accuracy of no worse than 1%. The flow meter was installed between the receiver and the suction fan.

Smoke was supplied to the flow by a smoke generator Safex (MT-Gravity fluid with medium fog density). The smoke particles size varied from 0.1 to 5 μm. To provide uniform flow seeding, the smoke preparation chamber with the volume of 0.864 m^3 was mounted upstream of the measurement section inlet. The smoke was supplied through the chamber's sidewall at the distance of 1 m from the inlet.

Smoke visualization was recorded by a monochrome high-speed camera Fastec HiSpec with a high-aperture lens Navitar. Continuous-wave DPSS laser KLM-532/5000-h was used for light sheet generation. The highest laser power was 5 W.

3. Test measurements

To provide the measurement reliability, test measurements of steady flow parameters were performed prior to measurements in the unsteady flow. Streamwise and transverse velocity fluctuation components were measured in the gaps between ribs no. 1-2, 2-3, 3-4, and 4-5. The results were compared to paper [15]. SIV technique was employed. The framing frequency was 4000 fps, exposure time 20 μs, scaling factor 19.2 pix/mm, reference interrogation window size 32×8 pix^2, number of processed frames in each video 15000. Flow in the channel symmetry plane was recorded. The measurement results are plotted in figure 2. They agree well with the results obtained by other measurement methods after the third rib. This suggests the conclusion that the flow in the measurement plane is two-dimensional and typical of rib-roughened channels. The conclusion on flow two-dimensionality in this case is based on the well-known fact that the flow near the rib-roughened wall can be considered fully developed starting from the third rib, and the flow near the smooth wall of the same channel – starting from the 6th rib [16].

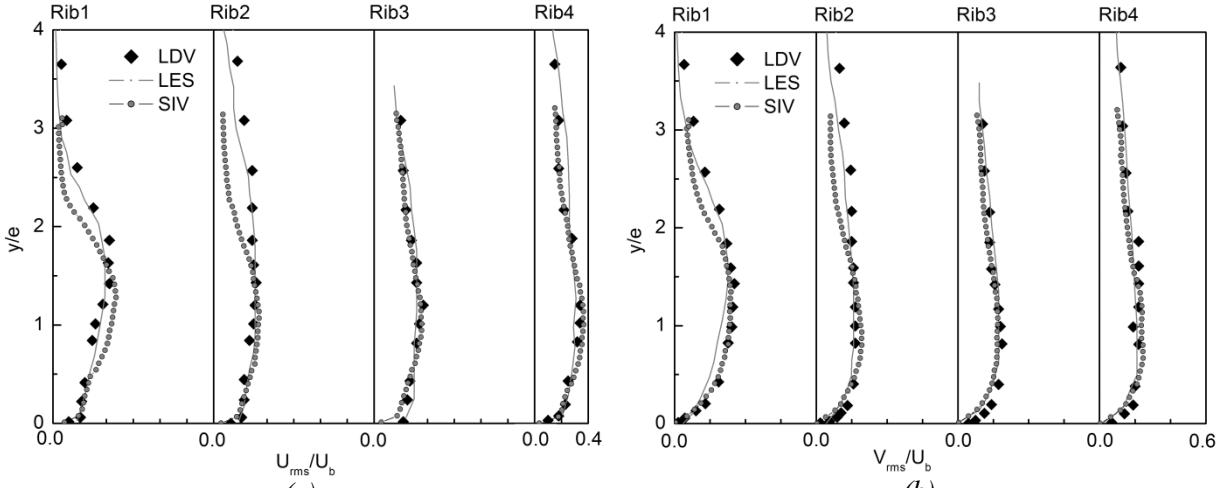

Figure 2. Profiles of streamwise (*a*) and transverse (*b*) velocity fluctuations. LDV and LES [15]

4. Results and discussion

Kinematic structure of unsteady turbulent flow has been studied using the high-speed smoke visualization. 22 flow regimes have been examined spanning a wide range of frequency and amplitude of flow rate pulsations. The analysis of the obtained data showed that the latter can be divided into groups with common features, and presentation of the groups in β, Sr coordinates can predict their occurrence (figure 3).

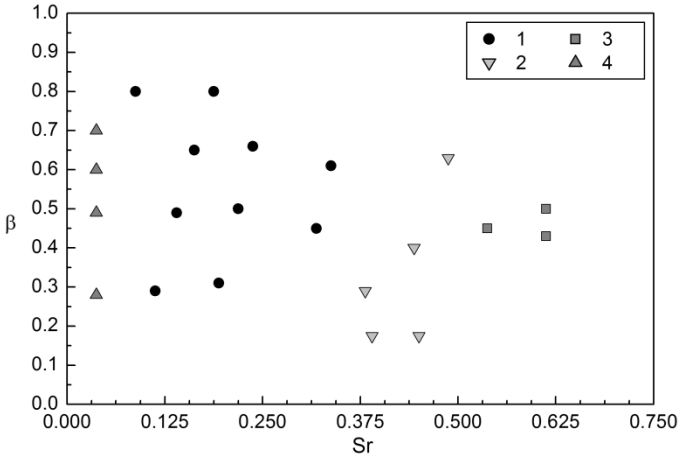

Figure 3. Flow map: 1 – resonance; 2 – transitional; 3 – high-frequency; 4 – low-frequency.

Four flow patterns have been revealed: low-frequency, resonance, transitional and high-frequency. Their features are schematically shown in figure 4.

Low-frequency flow pattern (figure 4, *a*) is characterized by the largest vortex *II* formed behind the rib. It starts forming in the flow acceleration phase when the gas flows into the leeward region behind the rib along the trajectory *a*. Initially the vortex dimensions are comparable to the rib height. This vortex is outlined by curve *b*. In the remaining part of the gap between the ribs the flow is swept downstream and the gas is replaced by new portions down to the region of viscous sublayer. In the freestream deceleration phase, the formed vortex gradually grows reaching 3-4 rib heights (the vortex is outlined by curve *c*) with proportional reduction in rotation velocity. In the vicinity of the minimum freestream velocity the vortex almost comes to a halt and disintegrates. A separation region is formed in front of the rib in the flow acceleration phase. Its streamwise dimension is about 1.5 rib heights. This region collapses in the flow deceleration phase.

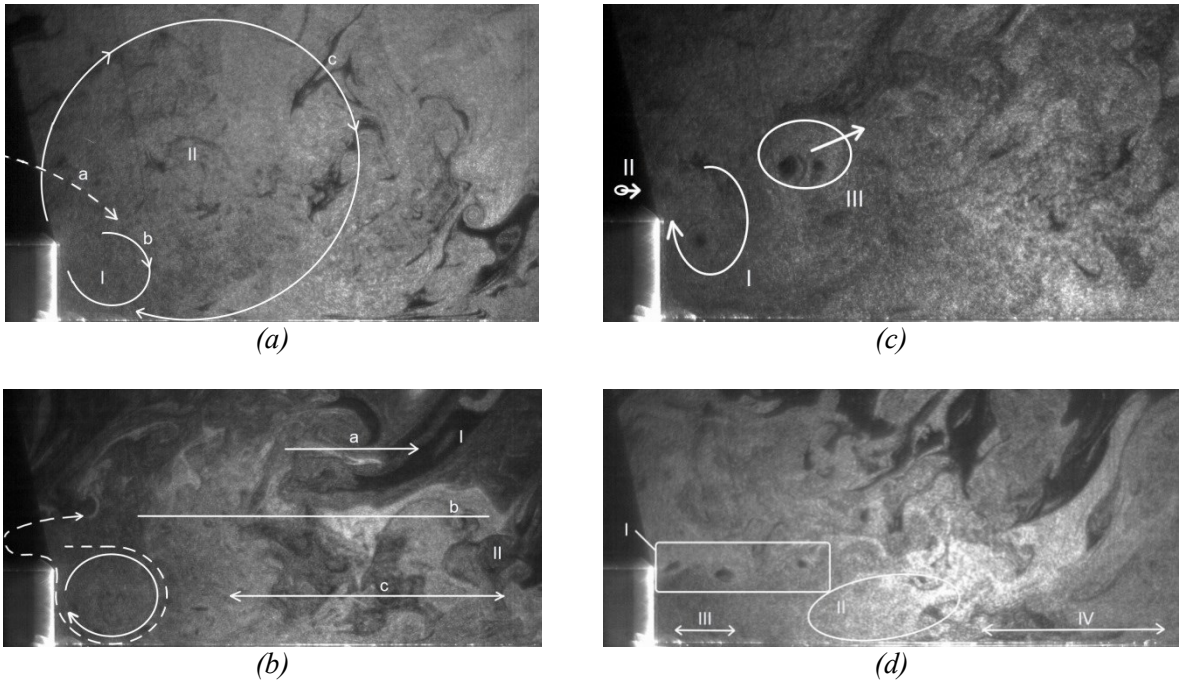

Figure 4. Flow patterns: *(a)* – low-frequency; *(b)* – resonance; *(c)* – transitional; *(d)* – high-frequency

In the resonance regime (figure 4, *b*), the gas above the ribs (region *I*) typically moves like a solid body along the trajectory *a*. Moreover, the region boundary can be visually observed (line *b*) below which the gas swings actively along the line *c*. The swing is due to the effect of the downstream rib and the gas viscosity. Moreover, while in the region *I* the velocity reduces to zero in the flow deceleration phase, the reverse flow is observed in the region *II* along the whole channel wall.

There is no classic recirculation region behind the rib in the resonance regime. Instead, a strong vortex with the size of about the rig height is formed in the flow acceleration phase. In the flow deceleration phase this vortex is displaced upstream by the oscillating gas contributing to the intense mass transfer on the rib surface. The gas moves along the dotted line (figure 4, *b*). When the velocity amplitude is high, the vortex trajectory changes so that it moves along almost the whole rib surface including the rib front face. Thus, in this case of periodic entrainment of vortex to the region in front of the rib, no separation region is formed in this zone.

In the high-frequency regime (figure 4, *d*) a street of small vortices is shed from the rib edge (region *I*) and moves parallel to the channel axis. It leads to the displacement of the mixing zone behind the rib (region *II*) further downstream and the formation of stagnation region *III* immediately behind the rib. This stagnation region exhibits extremely weak mass transfer to the core flow. In the near-wall region downstream of the flow reattachment the mass transfer due to the near-wall layer oscillations is also weak (region *IV*). There is no separation region in front of the rib apart from a small corner vortex.

The transitional regime is in many ways similar to the resonance regime but the vortex that moves past the rib is considerably weaker. At the same time, the features of high-frequency regime are observed near the rib's trailing edge. Superposition of these two regimes leads to formation of the street of vortex pairs. The latter are formed according to the following mechanism. In the flow acceleration phase, the flow moves near the rib surface along the trajectory *I* (figure 4, *c*). This leads to formation of a vortex that is half the rib height in size. In the flow deceleration phase, this vortex starts moving up along the rib wall similarly to the resonance regime. But approaching the rib edge it meets the vortex *II* of the same size formed at the rib edge. Then the inertia of the first vortex pushes the vortex pair out to the core flow. This process occurs at the very beginning of the flow acceleration phase. During the rest of the flow acceleration phase, the vortex pair (region *III*) moves with the flow as a whole and disintegrates in the deceleration phase. In the remaining part of the channel the fluid motion is similar to the resonance regime.

Conclusions

SIV measurements of the profiles of velocity fluctuations have been performed in the gaps between the ribs in the entrance region of the rib-roughened channel. The measurements have been performed in the steady regime. It has been demonstrated that the two-dimensional flow typical of rib-roughened channels occurs in the considered channel. Then the effect of flow rate pulsations on the flow pattern has been studied using high-speed smoke visualization of flow. Different frequencies and amplitudes of harmonic flow rate pulsations have been considered. The obtained data yielded qualitative classification of flow patterns, and the presentation of these data in β, Sr coordinates allows prediction of the flow pattern depending on the initial data. For the flow regimes other than the steady ones, a detailed description of time evolution of the kinematic flow structure is provided with the focus on mass transfer in the near-wall region and around the ribs.

Acknowledgments

This study was financially supported by Russian Foundation for Basic Research and the Government of the Republic of Tatarstan (project No. 17-48-160658).

References

[1] Gortyshov Yu F, Popov I A, Olimpiev V V, Schelchkov A V, Kaskov S I 2009 *Thermohydraulic performance of advanced methods of heat transfer enhancement in the ducts of heat transfer equipment* (Kazan: Center Innovacionnikh Tehnologiy) p 530 *(in Russian)*
[2] Xie G, Zheng S, Zhang W, Sunden B 2013 *Applied Thermal Engineering* **61** 289–300
[3] Moon M, Park M, Kim K 2014 *International Journal of Heat and Mass Transfer* **71** 275–284
[4] Davletshin I, Mikheev N 2012 *High Temperature* **50** 412–419
[5] Cukurel B, Selcan C, Stratmann M 2015 *International Journal of Heat and Mass Transfer* **52** 2223–2235
[6] Saric S, Jakirlic S, Tropea C 2005 *Journal of Fluids Engineering* **127** 879–887
[7] Das Gupta A, Zhao P, Ray S 2016 54th AIAA Aerospace sciences Meeting *(San Diego)* vol 5 (NY: Red Hook)
[8] Chun K, Sung H 1996 *Exp. Fluids* **21** 417–426
[9] Yoshioka S, Obi S, Masuda S 2001 *International Journal Heat and Fluid Flow* **22** 301–307
[10] Coletti F, Cresci I, Arts T 2013 *International Journal of Heat and Fluid Flow* **44** 181–196
[11] Cardwell N, Vlachos P, Thole K, 2011 *Exp. Fluids* **50** 1357–1371
[12] Mikheev N I and Dushin N S 2016 *Instruments and Experimental Techniques* **59** 880–887
[13] Mikheev N I, Goltsman A E, Saushin I I, Dushina O A Estimation of turbulent energy dissipation in the boundary layer using Smoke Image Velocimetry *Exp. Fluids* DOI: 10.1007/s00348-017-2379-x *(in press)*
[14] Dushin N S, Mikheev A N, Mikheev N I, Molochnikov V M 2014 *Instruments and Experimental Techniques* **57** 499-502
[15] Sewall E A, Tafti D K, Graham A B, Thole K A 2006 *International Journal of Heat and Fluid Flow* **27** 243–258
[16] Graham A B, Sewall E A and Thole K A 2004 *Proc. of ASME Turbo Expo (Vienna)* GT2004-53361